



**SIMULATION OPTIMIZATION SYSTEMS**  
Research Laboratory

**SOME PRACTICAL CONSIDERATIONS  
ON IMPLEMENTING NONLINEAR LARGE-SIGNAL  
FET EQUIVALENT CIRCUIT MODELS**

**J.W. Bandler, S. Ye and Q.J. Zhang**

**SOS-89-7-R**

**December 1989**

McMASTER UNIVERSITY  
Hamilton, Canada L8S 4L7  
Department of Electrical and Computer Engineering

THE UNIVERSITY OF CHICAGO  
LIBRARY  
540 EAST 57TH STREET  
CHICAGO, ILL. 60637  
TEL: 773-936-3000  
WWW.CHICAGO.EDU

**SOME PRACTICAL CONSIDERATIONS  
ON IMPLEMENTING NONLINEAR LARGE-SIGNAL  
FET EQUIVALENT CIRCUIT MODELS**

J.W. Bandler, S. Ye and Q.J. Zhang

SOS-89-7-R

December 1989

© J.W. Bandler, S.Ye and Q.J. Zhang 1989

No part of this document may be copied, translated, transcribed or entered in any form into any machine without written permission. Address enquiries in this regard to Dr. J.W. Bandler. Excerpts may be quoted for scholarly purposes with full acknowledgement of source. This document may not be lent or circulated without this title page and its original cover.



SOME PRACTICAL CONSIDERATIONS ON IMPLEMENTING NONLINEAR  
LARGE-SIGNAL FET EQUIVALENT CIRCUIT MODELS

J.W. Bandler, S. Ye and Q.J. Zhang

*Abstract* Two procedures are described which are employed to calculate the drain-to-source current sources of the two widely used nonlinear large-signal FET models, namely, the Materka and Kacprzak model and the Curtice model. Numerical examples show improvements in the behaviour and robustness of the FET models when the procedures are applied.

---

This work was supported in part by the Natural Sciences and Engineering Research Council of Canada under Grants STR0040923 and OGP0007239 and in part by Optimization Systems Associates Inc.

The authors are with the Simulation Optimization Systems Research Laboratory and the Department of Electrical and Computer Engineering, McMaster University, Hamilton, Canada L8S 4L7. J.W. Bandler and Q.J. Zhang are also with Optimization Systems Associates Inc., P.O. Box 8083, Dundas, Ontario, Canada L9H 5E7.

## I. INTRODUCTION

A good equivalent circuit model for FET devices is vital to microwave CAD. Over the years various nonlinear large-signal FET models have been proposed. Some of them have been successfully used in nonlinear circuit simulations and optimizations. The critical nonlinear component in these models is the drain-to-source nonlinear current source. This report discusses specific aspects on implementing the drain-to-source nonlinear current sources of two widely used models, namely, the Materka and Kacprzak model [1] and the Curtice model [2], from the programming point of view.

Section II describes certain aspects of implementing the (modified) Materka and Kacprzak model. The Curtice model is discussed in Section III. These two models have been implemented in the nonlinear microwave CAD program McCAE [3], where the models are used in the nonlinear harmonic balance simulation environment.

## II. THE MODIFIED MATERKA AND KACPRZAK MODEL

The intrinsic part of the Materka and Kacprzak FET model [1] is shown in Fig. 1, where the drain-to-source nonlinear current source  $i_D$  is characterized as

$$i_D = I_{DSS} \left[ 1 - \frac{v_G}{V_p} \right]^2 \cdot \tanh \left[ \frac{\alpha_D v_D}{v_G - V_p} \right], \quad (1)$$

where

$$V_p = V_{p0} + \gamma v_D.$$

The characteristics of  $i_G$ ,  $i_B$  and  $C_1$  can be found in [1].  $R_1$  and  $C_F$  are considered as linear elements.

To be more flexible, the model was later modified in Microwave Harmonica [4], where the characteristic of  $i_D$  becomes

$$i_D = F[v_G(t - \tau), v_D(t)] \left( 1 + S_S \frac{v_D}{I_{DSS}} \right), \quad (2)$$

where

$$F(v_G, v_D) = I_{DSS} \left[ 1 - \frac{v_G}{V_{p0} + \gamma v_D} \right]^{(E + K_E v_G)} \cdot \tanh \left[ \frac{S_1 v_D}{I_{DSS}(1 - K_G v_G)} \right]. \quad (3)$$

From the implementational point of view, direct use of (2) and (3) to calculate  $i_D$  may not be appropriate due to situations like unpredictable values of  $v_G$  and  $v_D$  during simulation, model parameter changes in model parameter extraction optimization, and so on. To avoid possible numerical difficulties, the following procedure is employed:

*Step 1*  $f_1 = \text{Max}[1 \times 10^{-6}, 1 - v_G/(V_{p0} + \gamma v_D)]$ .

*Step 2*  $f_2 = \text{Max}[1 \times 10^{-6}, E + K_E v_G]$ .

*Step 3*  $f_3 = \text{Min}[40, S_1 v_D / I_{DSS}(1 - K_G v_G)]$ , if  $S_1 v_D / I_{DSS}(1 - K_G v_G) \geq 0$ ,

and  $f_3 = \text{Max}[-40, S_1 v_D / I_{DSS}(1 - K_G v_G)]$ , if  $S_1 v_D / I_{DSS}(1 - K_G v_G) < 0$ .

*Step 4*  $f_4 = I_{DSS} + S_S v_D$ .

*Step 5*  $i_D$  is then

$$i_D = (f_1^{f_2}) \cdot \tanh(f_3) \cdot f_4. \quad (4)$$

It is not difficult to see in the procedure that  $f_1$  is used to avoid taking the exponential of negative or zero values, and  $f_2$  to avoid a negative exponent which is nonphysical.

#### *Example*

To illustrate the above procedure, consider  $i_D$  with parameter values taken from [5], i.e.,

$$\begin{array}{llll} I_{DSS} = 0.0740 & V_{p0} = -3.185 & \gamma = 0.0177 & E = 2.937 \\ K_E = -0.9077 & S_1 = 0.1527 & K_G = -0.4912 & S_S = 0.0022 \end{array} .$$

We calculate  $i_D$  by varying  $v_G$  from -3.5V to 2.0V with a step of 0.25V and  $v_D$  from 0 to 9.5V with a step of 0.5V.

Direct use of (2) and (3) results in the same values of  $i_D$  as by using (4) when  $v_G$  is between -2.0V to 2.0V. However, using (2) and (3), we obtained negative  $i_D$  values when  $v_G$  is below -2.25V and  $v_D > 0$ , which is non-physical. An "Undefined exponential" error occurred when  $v_G = -3.25V$ . None of these phenomena occur when we use (4) to calculate  $i_D$ .

### III. CURTICE MODEL

Fig. 2 depicts the intrinsic part of the Curtice model [2]. Similar to the discussions on the Materka and Kacprzak model, we only consider the nonlinear current source  $i_D$ , which is characterized as

$$i_D = (A_0 + A_1 v_1 + A_2 v_1^2 + A_3 v_1^3) \cdot \tanh(\gamma v_D) \quad (5)$$

where

$$v_1 = v_G [1 + \beta(V_{DS0} - v_D)] .$$

Assume that  $i_D$  is non-negative and  $i_D$  is a monotonically increasing function of  $v_G$  if  $v_D$  has a fixed positive value. From the definition given in (5)  $i_D$  is a cubic function of  $v_G$  when  $v_D$  is fixed. Depending on different values of the coefficients and the actual  $v_D$ , the relationship between  $i_D$  and  $v_G$  behaves in one of the typical forms shown in Fig. 3.

To insure that  $i_D$  is always physical, an intuitive procedure has been developed to compute  $i_D$ . The main objective is to eliminate part(s) of the cubic curve which may not have any physical meaning. The procedure is as follows.

*Step 1* Let  $i_D = K(a_0 + a_1 v_G + a_2 v_G^2 + a_3 v_G^3) \cdot \tanh(\gamma v_D)$ , and solve  $v_G$  from  $\partial i_D / \partial v_G = 0$ .

*Step 2* If there are no two distinct real solutions,  $i_D$  is a monotonic function of  $v_G$ . We compute  $i_D$  using (5).

If there are two distinct real solutions  $v_{G1}$  and  $v_{G2}$  with  $v_{G1} < v_{G2}$ , and  $a_3 < 0$  which corresponds to Fig. 3(c),  $i_D$  is calculated by

$$\begin{aligned} i_D &= i_D(v_G, v_D), & \text{if } v_{G1} < v_G < v_{G2} \\ i_D &= i_D(v_{G1}, v_D), & \text{if } v_G \leq v_{G1} \\ i_D &= i_D(v_{G2}, v_D), & \text{if } v_{G2} \leq v_G . \end{aligned}$$

If there are two distinct real solutions  $v_{G1}$  and  $v_{G2}$  with  $v_{G1} < v_{G2}$ , and  $a_3 > 0$  which corresponds to Fig. 3(d),  $i_D$  is calculated by

$$i_D = i_D(v_G, v_D), \quad \text{if } v_{G2} < v_G$$



$$i_D = i_D(v_{G2}, v_D), \text{ if } v_G \leq v_{G2} .$$

*Step 3* If  $i_D < 0$  and  $v_D > 0$ , set  $i_D = 0$ .

If  $i_D > 0$  and  $v_D < 0$ , set  $i_D = 0$ .

*Example*

Similarly to the example discussed in Section II,  $i_D$  in the Curtice model is calculated with  $v_G$  from -3V to 2V with a step of 0.5V and  $v_D$  from 0 to 9.5V with a step of 0.5V. The parameters of  $i_D$  are taken from [2]

$$\begin{aligned} A_0 &= 0.05185 & A_1 &= 0.004036 & A_2 &= -0.009478 & A_3 &= -0.009058 \\ \beta &= 0.04062 & \gamma &= 1.608 & V_{DS0} &= 4.0 \end{aligned}$$

Fig. 4 shows the results obtained by direct use of (5). It can be seen in this example that when  $v_G > 1.0V$  or  $v_G \leq -2.0V$ , the model behaves non-physically. Fig. 5 illustrates the  $i_D$  characteristics obtained by using the procedure presented in this section, where  $v_G$  and  $v_D$  have the same ranges as in Fig. 4. Significant improvement can be observed.

#### IV. CONCLUSIONS

In this report, practical implementations of the modified Materka and Kacprzak and the Curtice nonlinear large-signal FET models have been presented. Examples have demonstrated that with our calculation procedures, the behaviour of the model can be improved and the model can be more physically robust.

The procedures presented in this report have been implemented and tested in the program McCAE. McCAE has successfully employed the FET models for harmonic balance simulation and optimization.

## REFERENCES

- [1] A. Materka and T. Kacprzak, "Computer calculation of large-signal GaAs FET amplifier characteristics", *IEEE Trans. Microwave Theory Tech.*, vol. MTT-33, 1985, pp. 129-135.
- [2] W.R. Curtice, "GaAs MESFET modeling and nonlinear CAD", *IEEE Trans. Microwave Theory Tech.*, vol. 36, 1988, pp. 220-230.
- [3] *McCAE*, Simulation Optimization Systems Research Laboratory and Department of Electrical and Computer Engineering, McMaster University, Hamilton, Canada, L8S 4L7, 1989.
- [4] *Microwave Harmonica User's Manual*, Compact Software Inc., Paterson, NJ, 07504, 1987.
- [5] J.W. Bandler, Q.J. Zhang, S. Ye and S.H. Chen, "Efficient large-signal FET parameter extraction using harmonics", *IEEE Trans. Microwave Theory Tech.*, vol. 37, 1989, pp. 2099-2108.

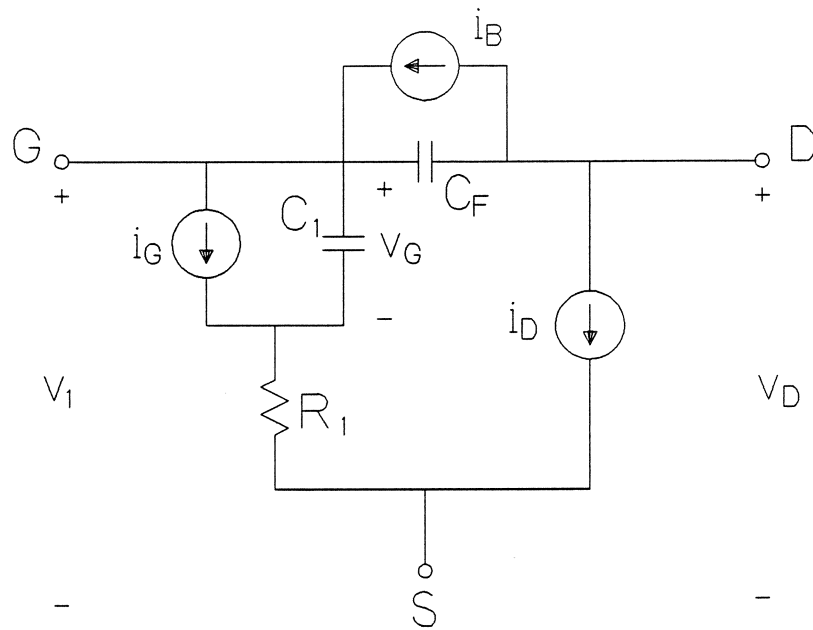


Fig. 1 Intrinsic part of the (modified) Materka and Kacprzak FET model.

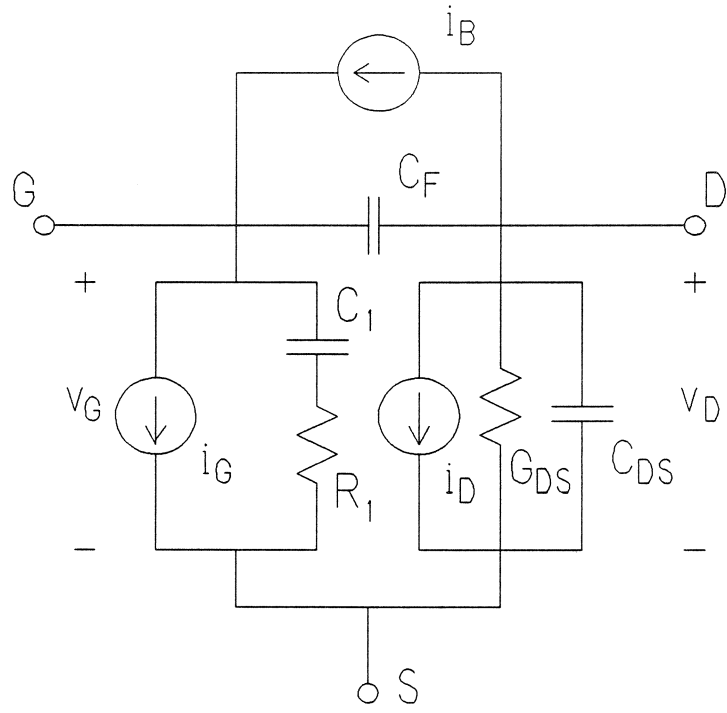


Fig. 2 Intrinsic part of the Curtice FET model.

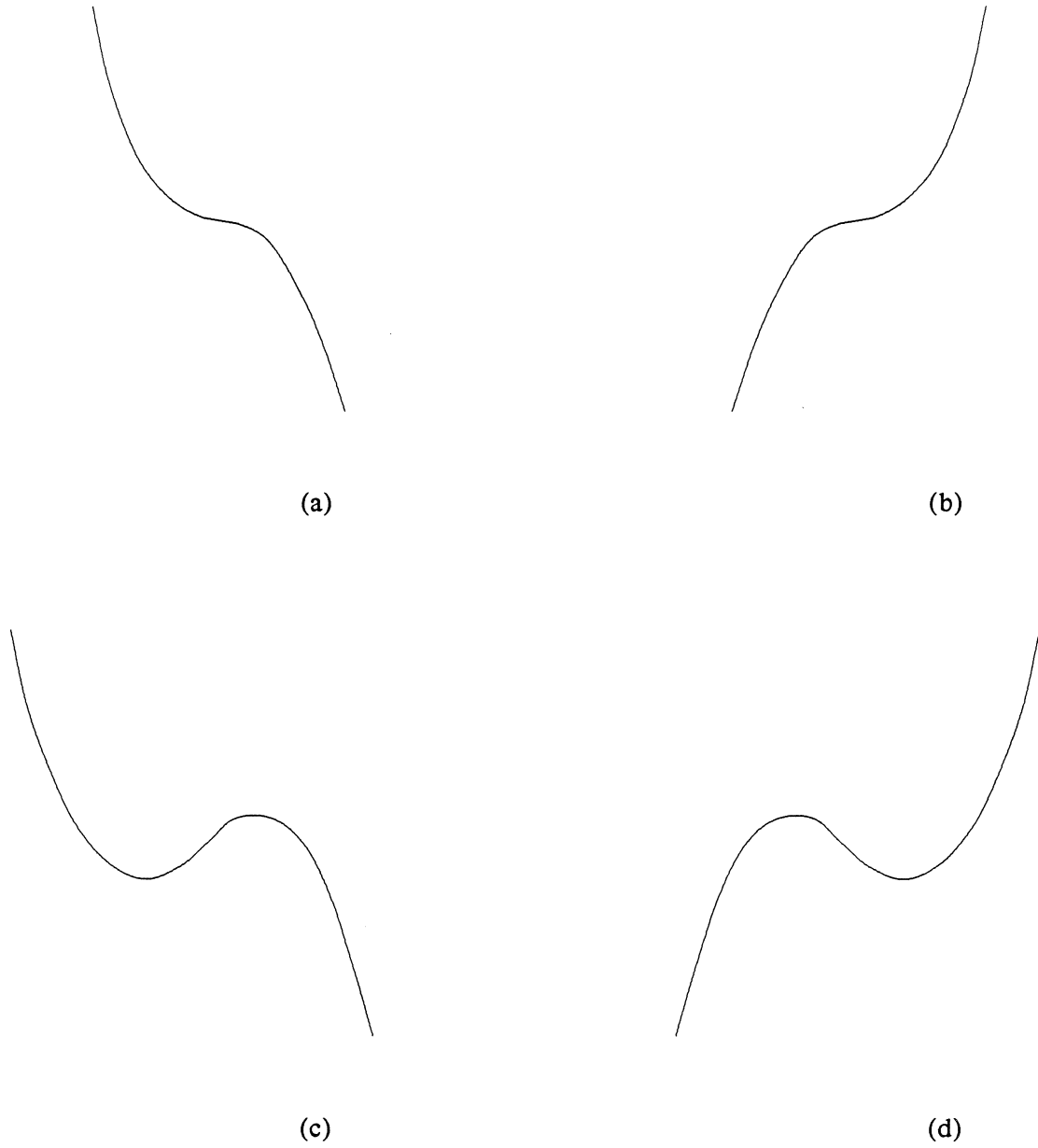


Fig. 3 Possible  $i_D$  w.r.t.  $v_G$  characteristics. When we solve  $\partial i_D / \partial v_G = 0$  for  $v_G$ , which is equivalent to  $a_1 + a_2 v_G + a_3 v_G^2 = 0$ , (a) no two distinct real solutions and  $a_3 < 0$ ; (b) no two distinct real solutions and  $a_3 > 0$ ; (c) two different real solutions and  $a_3 < 0$ ; (d) two real solutions and  $a_3 > 0$ .

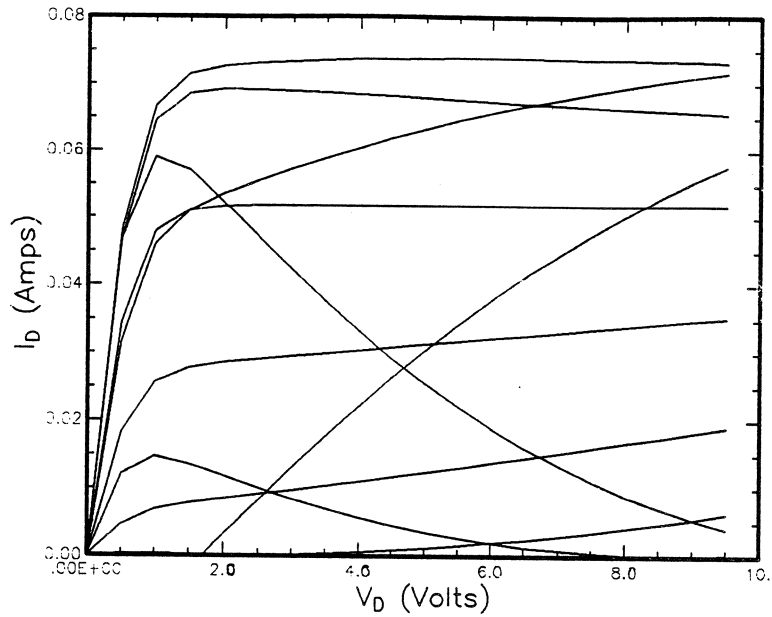


Fig. 4 The characteristics of  $i_D$  in the Curtice FET model w.r.t.  $v_G$  and  $v_D$  obtained by using (5), where  $v_G$  is from -3V to 2V with a step of 0.5V, and  $v_D$  is from 0 to 9.5V with a step of 0.5V.

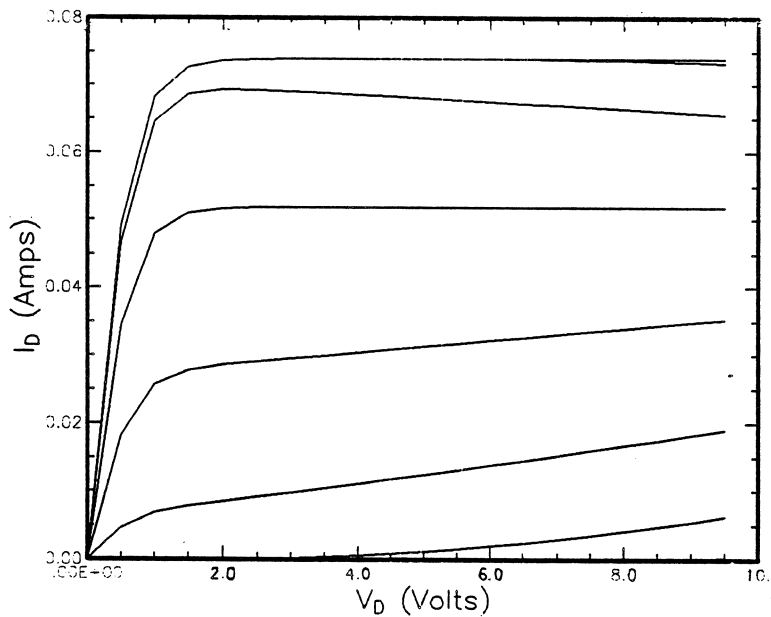


Fig. 5 The characteristics of  $i_D$  in the Curtice FET model w.r.t.  $v_G$  and  $v_D$  obtained by using the procedure presented in Section III, where  $v_G$  is from -3V to 2V with a step of 0.5V, and  $v_D$  is from 0 to 9.5V with a step of 0.5V.



